View Article Online
View Journal

ChemComm

Chemical Communications

Accepted Manuscript

This article can be cited before page numbers have been issued, to do this please use: J. Agin-Gontarek, W. Wróblewski, H. Sakurai and A. Kasprzak, *Chem. Commun.*, 2026, DOI: 10.1039/D6CC02933G.

ROYAL SOCIETY
OF CHEMISTRY

rsc.li/chemcomm

ChemComm

View Article Online
DOI: 10.1039/D6CC02933G

COMMUNICATION

Switching Cation Selectivity via Steric Tuning in Sumanene-Based Receptors

Received 00th January 20xx,
Accepted 00th January 20xx

DOI: 10.1039/x0xx00000x

Joachim Ażgin-Gontarek,[a] Wojciech Wróblewski,[a] Hidehiro Sakurai,[b,c] and Artur Kasprzak[a]*

Steric control of metal cation selectivity in curved π-systems based on sumanene scaffold is reported. In comparison to variety of examples of Cs$^+$-oriented sumanene receptors, herein we show that increasing the steric hindrance of the receptor part enables tuning the recognition of metal cations, including the unprecedented design of sumanene-based lead(II) receptor.

Buckybowls are emerging class of molecules not only as scaffolds of organic materials with attractive bowl-shaped structures and unique properties, but also in terms of designing functional organic molecules for various applications.[1–7] One of the leading examples of buckybowls is a C_3-symmetric sumanene[8,9] (**1**; **Fig. 1**) composed of four hexagonal and three pentagonal rings, which was first synthesized (2003) almost 40 years after C_{5v}-symmetric corannulene[10,11]. In the last 15 years, chemistry and properties of sumanene were intensively explored, revealing attractive possibilities of this scaffold for π-expanded bowl-shaped organic molecules[12–16], and as a ligand in organometallic complexes[17–21] and organized organic materials[22–24].

During the last 7 years, our group reported on the attractive properties of sumanene for designing molecular receptors of metal cations, mostly for cesium cations (Cs$^+$) optical or electrochemical detection.[25–32] This non-covalent interaction is driven by the formation of dynamic cation-π interactions between a metal cation and π-electrons from a sumanene bowl.[33–36] The selective detection of Cs$^+$ by sumanene receptors results from the site-specific non-covalent interactions between concave site of sumanene bowl, which size matches perfectly with the Cs$^+$ van der Waals radius.[37] Only several sumanene derivatives monosubstitued at the aromatic position with 1,2,3-triazole skeletons[38], 1,1,2,2-tetraphenylethene units[39] or bis(terpyridine)ruthenium(II) complexes[40] featured exclusive lithium cations (Li$^+$) selectivity, which was hypothesized to include sumanene's convex-oriented complexation.

We identified tuning metal cation selectivity of sumanene receptors by means of careful steric control of the cation-π interactions of the receptor side as an attractive concept to further advance sumanene receptors science. Inspired by the structure of the bis-sumanene derivative monosubstituted at the aromatic position with the 1,2,3-triazole moiety, which featured lithium cations (Li$^+$) selectivity[38] (**2**; **Fig. 1**), as well as taking into account the easiness of introducing triazole moieties by means of *click reaction*, herein we report on the synthesis of series of triazole-functionalized sumanenes (**3**-**6**; **Fig. 1**), differing in the steric hindrance of the receptor part of the molecule (sumanene bowl in conjunction with the 1,2,3-triazole skeleton). By extensive spectrofluorimetric and potentiometric studies, we demonstrated that thanks to the steric tuning and the direct conjunction of receptor properties of triazole and sumanene scaffolds in the molecule, these newly designed receptors featured enhanced selectivity towards small alkali cations (lithium, Li$^+$) up to d- (copper(II), Cu^{2+}) and p-block metal cations, with the first lead(II) (Pb^{2+}) oriented sumanene receptors (**Fig. 1**). As a result, this study constitutes a valuable contribution to the further growth of curved π-conjugated receptors science with tunable affinity properties.

The synthesis of target sumanene receptors **3**-**6** (**Fig. 1**) was based on the 1,3-dipolar copper-catalyzed azide-alkyne cycloaddition (CuAAC) reaction between 2-ethynylsumanene (**7**)[27] and respective aromatic azides bearing the 1,3,5-triphenylbenzene motif (**8**-**11**; refer to Electronic Supporting Information (ESI), Sections S1-S3, for the full experimental details and compounds characterization data). Azides **8**-**11** were synthesized under mild conditions from corresponding

---

[a] *Faculty of Chemistry, Warsaw University of Technology, Noakowskiego Str. 3, 00-664 Warsaw, Poland*
* *Corresponding author e-mail: artur.kasprzak@pw.edu.pl (A.K.)*
[b] *Division of Applied Chemistry, Graduate School of Engineering, The University of Osaka, 2-1 Yamadaoka, Suita, 565-0871 Osaka, Japan*
[c] *Innovative Catalysis Science Division, Institute for Open and Transdisciplinary Research Initiatives (ICS-OTRI), The University of Osaka, Suita, Osaka 565-0871, Japan*

† Footnotes relating to the title and/or authors should appear here. Electronic supporting information (ESI): Materials and methods, experimental procedures, compounds characterization data, data on receptor studies, DFT computational details.

View Article Online
DOI: 10.1039/D6CC02933G

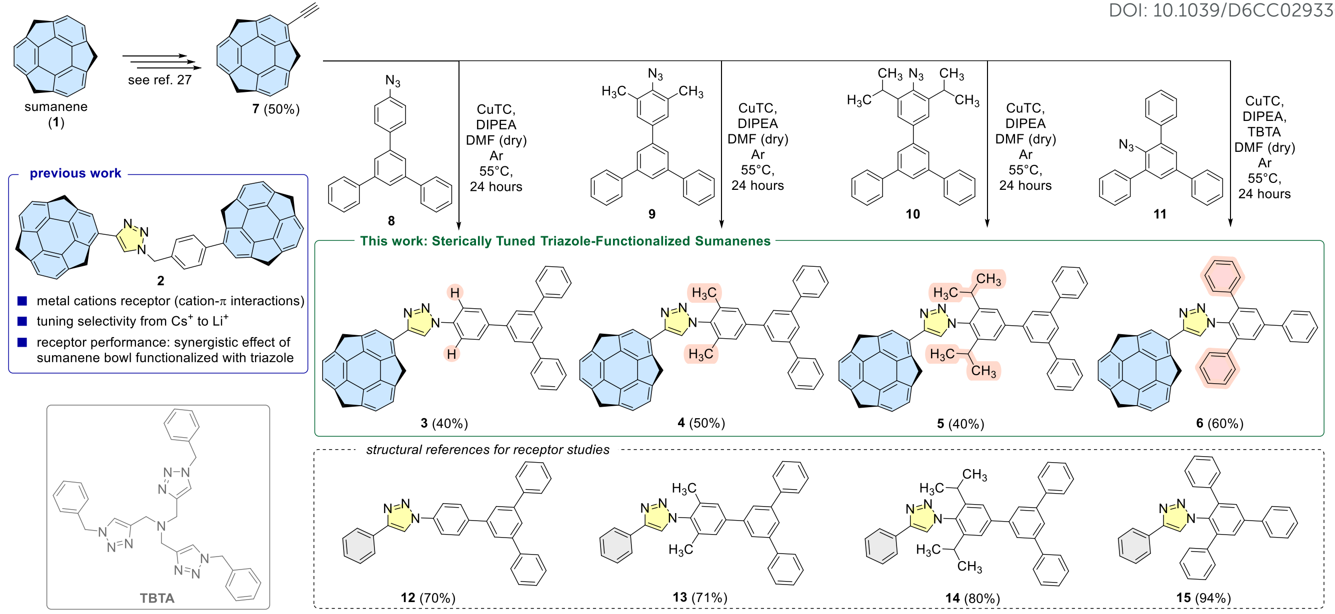

Fig. 1 Synthesis of receptors **3**-**6** and the presentation of the contents of this work.

aromatic amines by means of the diazotization reaction[41,42] ($NaNO_2$, HCl) followed by the treatment with sodium azide (**Fig. 1**). Starting aromatic amines were synthesized using the Suzuki-Miyaura cross-coupling between (*i*) 2-([1,1':3',1''-terphenyl]-5'-yl)-4,4,5,5-tetramethyl-1,3,2-dioxaborolane[43] and 2,6-disubstituted 4-bromoanline derivatives (in the case of azides **9**-**10**) or (*ii*) phenylboronic acid and 2,4,6-tribromoanline[44] (in the case of azide **11**; see ESI, Section S1, for the reaction schemes).

In brief, the conditions for the synthesis of receptors **3**-**5** included the usage of copper(I) thiophene-2-carboxylate (CuTC) as the copper source, and *N*,*N*-diisopropylethylamine (DIPEA) in dry *N*,*N*-dimethylformamide (DMF) under argon atmosphere (24 hours, 55°C), providing the target products in good yields (40-60 %) after chromatographic purification. Interestingly, translating such conditions to the synthesis of receptor **6**, or using other widely employed catalytic systems (see optimization table in ESI, Section S1), did not provide the target product (no triazole product was formed). We concluded that the most plausible reason is the steric hindrance related to the azide group within the starting material **11** structure. To overcome this severe limitation, we used tris((1-benzyl-1*H*-1,2,3-triazol-4-yl)methyl)amine (TBTA) as a ligand for the process, taking into account previous reports on its usage in CuAAC reactions.[45,46] To our delight, employing CuTC, DIPEA in dry DMF (argon atmosphere, 24 hours, 55°C) provided target receptor **6** in good yield (60%; chromatographic purification on neutral alumina (Al_2O_3) as the stationary phase was required).

Additionally, to provide structural reference to the designed sumanene-based molecules **3**-**6** for further receptor assays, our synthetic studies also included the preparation of respective molecules featuring the presence of the phenyl substituent at the 4-position the 1,2,3-triazole skeleton (molecules **12**-**15**; **Fig. 1**) instead of the sumanenyl group. These molecules were synthesized in high yields (70-94%) under similar conditions as those for their sumanene analogs. Similarly to the synthesis of sumanene receptor **6**, the successful synthesis of reference compound **15** also required the usage of TBTA as a ligand for the process, suggesting the general reactivity profile for starting azide **11** in the studied CuAAC process.

Successful isolation of all synthesized molecules was confirmed by 1D and 2D NMR, as well as HRMS. In brief, the most diagnostic change in terms of target receptors **3**-**6** was the presence of the signal coming from the C-**H** proton of the 1,2,3-triazole moiety, along with the disappearance of the -C≡C-**H** signal from the parent 2-ethynylsumanene (**7**).

Regarding photophysical characterization, absorption (λ_{abs}) and emission (λ_{em}) maxima for molecules **3**-**6** (in THF) were located between 240-330 nm and 388-390 nm, respectively (see ESI, Section S4, for the spectra). HOMO and LUMO were located mainly on the sumanene bowl and triazole-triphenylbenzene parts, respectively (see ESI, Section S7, for DFT-computed HOMO and LUMO distributions).

DFT computations (B3LYP[47]/6-311g(d,p)[48]) enabled the visualization (**Fig. 2**) of the increasing steric hindrance of the receptor part in molecules **3**-**6** (sumanene bowl in conjunction with the triazole moiety) in the following order (a substituent in the bracket refers to the group marked in light pink in **Fig. 1**): **3** (H) < **4** (CH_3) < **5** ($CH(CH_3)_2$) < **6** (C_6H_5). Discussed increase in steric hindrance also resulted in slightly higher bowl depth for molecule **6** (1.14 Å) in comparison to other sumanene derivatives (1.11-1.12 Å). Additionally, judging from the DFT-computed electrostatic surface potential (ESP) distributions for receptors **3**-**6** (**Fig. 2**), in general, triazole part features relatively similar ESP value for all molecules (*ca.* −58 kJ·mol⁻¹), whereas the ESP value for the convex site of sumanene bowl is *ca.* 5 kJ·mol⁻¹ higher for the receptor **6** (−35 kJ·mol⁻¹) in comparison to other molecules. Therefore, DFT computations revealed that the most steric tuning of the receptor part in molecule **6** also influenced its electronic properties.

View Article Online
DOI: 10.1039/D6CC02933G

The selectivity of cation recognition by the studied receptors was first studied in a heterogeneous system, i.e., the derivatives **3-6** were introduced into polymeric membranes made of plasticized poly(vinyl chloride), used as ion-sensitive layers in potentiometric sensors. This method enables the determination of the potentiometric selectivity coefficients shown in **Fig. 3** and collected in Table S3 (refer to ESI, Section S1.3, for experimental details). The presence of a small methyl substituent (receptor **4**) or its absence (**3**) in receptor structure did not significantly alter the selectivity patterns of the membranes. However, the derivatives **3** and **4** provided an enhanced selectivity towards Li^+ over the remaining alkali metal cations, compared to blank membranes. Similar potentiometric and spectroscopic results were previously reported for a 1,2,3-triazole-linked bis-sumanene derivative **2**[38], which confirm that the direct linkage of sumanene to the triazole ring favours lithium cation binding. Structural modification with isopropyl moieties in receptor **5** yielded an unprecedented and significant gain in Pb^{2+} and Ba^{2+} affinity of the membranes, simultaneously suppressing their selectivity towards lipophilic alkali metal cations. Furthermore, receptor **6** featuring a larger, sterically hindering phenyl substituents, displayed even higher affinity for Pb^{2+} cations, comparable to that of the highly lipophilic Cs^+ cation, while achieving superior Pb^{2+} selectivity over other transition metal cations relative to blank membranes.

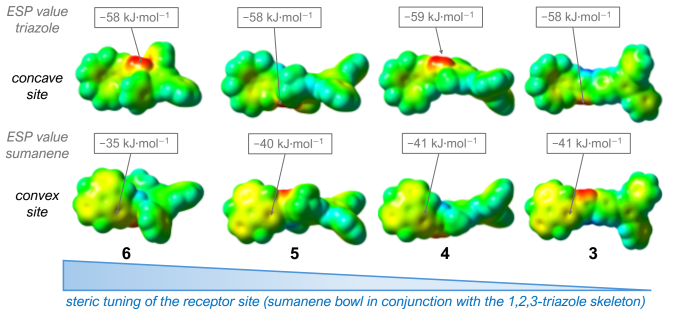

Fig. 2 DFT-computed (B3LYP/6-311g(d,p)) ESP plots for sumanene receptors **3-6** together with ESP values for triazole concave site and sumanene convex site.

Different selectivity pattern of receptors **3-6** might suggest that steric tuning resulted in an increased affinity towards Pb^{2+} which is a softer Lewis acid with a larger ionic radius, and which also features a stereochemically active $6s^2$ lone electron pair accessible for coordination.[49] The most notable preference of binding soft Pb^{2+} cations by receptor **6** in the series of tested receptors **3-6** might be supported with the highest ESP value for the convex site of the sumanene bowl for this receptor (**Fig. 2**). It is hypothesized that the combination of steric shielding of the concave site with the steric bulk, which is most significantly increased for **6** (see **Fig. 2**), enhanced the accessibility of the convex π-surface of the sumanene bowl, thereby favouring larger, more polarizable cations. This outcome suggests new modes of interaction for receptor **6** in comparison to variety examples of reported of Cs^+-selective sumanene receptors.

Additional experiments were carried out to evaluate the role of the sumanene bowl in cation binding by the receptors **3-6**. The selectivity coefficients of membranes doped with reference, truncated derivatives **12-15** of the studied sumanene-based receptors were similar to those of the blank membranes (see Fig. S52 and Table S4, ESI). Thus, the presence of the bowl-shaped sumanene motif in the receptor structure is crucial to tune the selectivity of the ion-sensitive layers. The only effect that could be attributed to coordination properties of the 1,2,3-triazole moiety was a slightly elevated affinity towards lithium and some divalent metal cations, notably in the case of derivative **13**. Based on the comparison of the selectivity of membranes containing **3-6** and **12-15** derivatives, it can be concluded that drastic changes in the membrane selectivity can be only obtained by introducing the curved sumanene unit to the truncated derivatives functionalized with bulky substituents exhibiting unique binding environment.

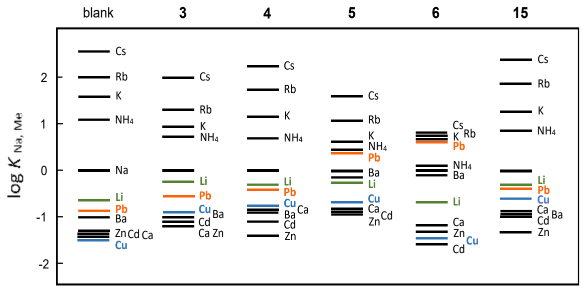

Fig. 3 Graphical presentation of the selectivity (values of log $K_{\text{Na, Me}}$) of PVC/o-NPOE membranes formulated with receptors **3-6** and **15** (10 mol% KTFPB) and without receptor (blank membrane); mean values were calculated for 3 electrode specimens.

The binding properties of the studied receptors **3-6** were further examined in solution (H_2O:THF = 1:1 v/v) using fluorescence spectroscopy. Taking into account the potentiometric results, fluorescence spectra titrations were performed against selected metal cations, namely: Li^+, Cu^{2+} and Pb^{2+} (refer to ESI, Section S1.4, for details of the spectrofluorimetric experiments). A systematic enhancement of fluorescence intensity was observed upon the addition of increasing molar equivalents of metal cations, however, the signal increase varied depending on the specific cation and the receptor studied (see **Fig. 4** for the titration for **6-Pb^{2+}** system; for other titrations see ESI, Figs. S53-S73).

Benesi-Hildebrand linear fitting of fluorescence titration data demonstrated a 1:1 stoichiometry of the metal cation complexes of receptors **3-5** and provided the estimation of respective association constants (*K*; Table S5, ESI). The receptor **3** exhibited increased affinity towards Li^+ and Cu^{2+}, whereas the derivative **5** towards Cu^{2+} and Pb^{2+} cations. Moreover, while derivative **3** exhibited the highest association constants overall, an exception was noted for Pb^{2+} cations; in this case the Pb^{2+} affinity progressively increased in the order of derivatives **3** < **4** < **5**. Notably, a similar enhancement of the Pb^{2+} selectivity was reflected during the potentiometric experiments.

The titration of receptor **6** with Li^+ cations resulted in no detectable changes in the emission signal, suggesting no interaction occurred. The loss of Li^+ potentiometric selectivity was also remarked for the membrane doped with this derivative (affinity for Li^+ cations matched the level observed for the blank membrane). Moreover, only minor changes in the fluorescence signal were measured during the titration of receptor **6** with K^+ or Cs^+ cations, indicating a low binding affinity toward both ions (Figs. S80-S81, ESI). On the other hand, the highest changes in intensity of the fluorescence signal of **6** were observed upon addition of Pb^{2+} cations (Figs. S74-S77, ESI). These results suggest that increase in steric hindrance of the binding site favours the complexation of bigger cations (Pb^{2+}) as opposed to smaller cations (Li^+). Furthermore, given the unsatisfactory fitting provided by the Benesi-Hildebrand plot, the titration data for receptor **6** were subsequently analysed using the non-linear data analysis (global fitting) tool *Bindfit*,[50–52] which revealed a good fit of the experimental data for 2:1 receptor-cation binding model (Figs. S78-S81, ESI), with comparable *K* values on the level of 10^5 M^{-1} for both Cu^{2+} and Pb^{2+} cations. Although deciphering the exact binding mode is not possible at this stage of the project, highly consistent potentiometric and fluorometric experimental data demonstrate emerging recognition mode for receptor **6**. This mechanism differs from those of known Cs^+-selective sumanene probes, which prefer Cs^+ coordination at the concave face of the bowl. Instead, for receptor **6**, it may involve a convex-oriented, sandwich-type binding mode driven by steric constraints, which aligns with the DFT-predicted convex-oriented interaction based on ESP distribution (**Fig. 2**) and interaction energies for concave- and convex-oriented **6**-Pb^{2+} systems.

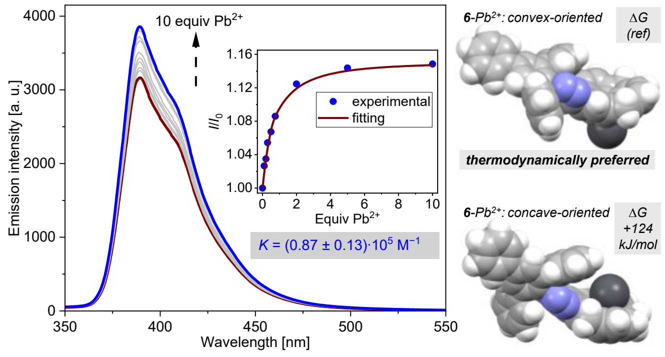

Fig. 4 (**left**) Emission spectra of receptor **6** in the presence of various amounts (equivalents = eq) of Pb^{2+} cations (λ_{ex} = 292 nm; THF:water = 1:1 v/v, C_6 = 0.02 mM). The inset shows global fitting (Bindfit) regarding these interactions ($K = (8.66 \pm 1.33)\cdot 10^4$ M^{-1}, model: 2:1 non-cooperative, covariance = $5.43\cdot 10^{-3}$); (**right**) DFT-computed **6**-Pb^{2+} systems with compared interaction energies (Δ*G*).

In conclusion, our work revealed the possibility of switching cation selectivity through steric modulation of curved π-surfaces of molecular receptors. In this regard, we demonstrated that triazole-functionalized sumanene receptors **3-6** featured distinct selectivity patterns attributed to the combined effect of the sumanene binding site and the specific substitution of the triazole-adjacent phenyl ring, increasing the steric hindrance of the binding site. Our approach resulted in the first, unpreceded lead(II) selectivity of sumanene receptor **6** with the most sterically hindered receptor site. We believe this work will highly stimulate future advances in programmable tuning ion selectivity in molecular receptors based on curved π-systems.

Acknowledgments

View Article Online
DOI: 10.1039/D6CC02933G

The financial supports from the National Science Centre, Poland, OPUS grant no. 2021/43/B/ST4/00114 (A.K.), Warsaw University of Technology (WUT, statutory support; A.K.), as well as JSPS KAKENHI (grant nos. JP21H05233 and JP24H00460; H.S.) are acknowledged. The computational studies were carried out with the support of the Interdisciplinary Centre for Mathematical and Computational Modelling University of Warsaw (ICM UW) under computational allocations no. G101-2385.

Authors Contributions

J.A. performed synthesis, characterization and receptor (potentiometric, spectroscopic) experiments under the supervision of A.K. and W.W. **W.W.** supervised potentiometric and spectrofluorimetric experiments by J.A., analysed the data, prepared manuscript text dealing with the potentiometric studies and spectrofluorimetric titrations, commented on the manuscript during the preparation of the final version. **H.S.** provided sumanene, funding for research from the Japanese side, and commented on the manuscript during the preparation of the final version. **A.K.** conceived the project, designed structures of all compounds, designed and supervised synthetic and spectrofluorimetric experiments by J.A., performed and processed DFT and TD-DFT computations, analysed the data, conceptualized and prepared the manuscript draft, compiled and prepared the supporting information, provided funding for research from the Polish side, corresponded with the Editor and Reviewers.

Conflicts of interest

There are no conflicts to declare.

Data availability

The data supporting this article have been included as part of the supplementary information.

References

1 Y. Chen and L. Zhang, *Acc. Chem. Res.*, 2025, **58**, 762–776.
2 X. Li, F. Kang and M. Inagaki, *Small*, 2016, **12**, 3206–3223.
3 M. Saito, H. Shinokubo and H. Sakurai, *Mater. Chem. Front.*, 2018, **2**, 635–661.
4 W.-S. Wong and M. Stępień, *Trends Chem.* 2022, **4**, 573–576.
5 A. Kasprzak, *Angew. Chem. Int. Ed.*, 2024, **63**, e202318437.
6 T. Amaya and T. Hirao, *Chem. Commun.*, 2011, **47**, 10524.
7 T. Amaya and T. Hirao, *Chem. Rec.*, 2015, **15**, 310–321.
8 H. Sakurai, T. Daiko and T. Hirao, *Science*, 2003, **301**, 1878–1878.
9 H. Sakurai, *BCSJ*, 2021, **94**, 1579–1587.
10 T. J. Seiders, E. L. Elliott, G. H. Grube and J. S. Siegel, *J. Am. Chem. Soc.*, 1999, **121**, 7804–7813.

View Article Online
DOI: 10.1039/D6CC02933G

11 W. E. Barth and R. G. Lawton, *J. Am. Chem. Soc.*, 1966, **88**, 380–381.

12 S. Alvi and R. Ali, *Beilstein J. Org. Chem.*, 2020, **16**, 2212–2259.

13 H. Toda, Y. Uetake, Y. Yakiyama, H. Nakazawa, T. Kajitani, T. Fukushima and H. Sakurai, *Synthesis*, 2019, **51**, 4576–4581.

14 N. Ngamsomprasert, Y. Yakiyama and H. Sakurai, *Chem. Lett.*, 2017, **46**, 446–448.

15 T. Amaya, T. Nakata and T. Hirao, *J. Am. Chem. Soc.*, 2009, **131**, 10810–10811.

16 T. Amaya, H. Sakane, T. Muneishi and T. Hirao, *Chem. Commun.*, 2008, 765–767.

17 M. A. Petrukhina, *Angew. Chem. Int. Ed.*, 2008, **47**, 1550–1552.

18 S. N. Spisak, Z. Wei, N. J. O'Neil, A. Yu. Rogachev, T. Amaya, T. Hirao and M. A. Petrukhina, *J. Am. Chem. Soc.*, 2015, **137**, 9768–9771.

19 T. Amaya, H. Sakane and T. Hirao, *Angew. Chem.*, 2007, **119**, 8528–8531.

20 T. Amaya and T. Hirao, in *Advances in Organometallic Chemistry and Catalysis*, ed. A. J. L. Pombeiro, John Wiley & Sons, Inc., Hoboken, NJ, USA, 2013, pp. 473–483.

21 T. Hirao, T. Amaya, T. Moriuchi, M. Hifumi, Y. Takahashi, I. Nowik and R. H. Herber, *J. Organomet. Chem.*, 2011, **696**, 3895–3899.

22 Y. Yakiyama, T. Hasegawa and H. Sakurai, *J. Am. Chem. Soc.*, 2019, **141**, 18099–18103.

23 I. Hisaki, H. Toda, H. Sato, N. Tohnai and H. Sakurai, *Angew. Chem. Int. Ed.*, 2017, **56**, 15294–15298.

24 H. Mizuno, H. Nakazawa, A. Miyagawa, Y. Yakiyama, H. Sakurai and G. Fukuhara, *Sci. Rep.*, 2024, **14**, 12534.

25 A. Kasprzak, A. Kowalczyk, A. Jagielska, B. Wagner, A. M. Nowicka and H. Sakurai, *Dalton Trans.*, 2020, **49**, 9965–9971.

26 A. Kasprzak and H. Sakurai, *Dalton Trans.*, 2019, **48**, 17147–17152.

27 A. Kasprzak, A. Gajda-Walczak, A. Kowalczyk, B. Wagner, A. M. Nowicka, M. Nishimoto, M. Koszytkowska-Stawińska and H. Sakurai, *J. Org. Chem.*, 2023, **88**, 4199–4208.

28 D. Ufnal, J. S. Cyniak, M. Krzyzanowski, K. Durka, H. Sakurai and A. Kasprzak, *Org. Biomol. Chem.*, 2024, **22**, 5117–5126.

29 A. Kasprzak and H. Sakurai, *Chem. Commun.*, 2021, **57**, 343–346.

30 A. Kasprzak, A. Tobolska, H. Sakurai and W. Wróblewski, *Dalton Trans.*, 2022, **51**, 468–472.

31 J. Ażgin, M. Wesoły, K. Durka, H. Sakurai, W. Wróblewski and A. Kasprzak, *Dalton Trans.*, 2024, **53**, 2964–2972.

32 Ł. Kurowski, J. S. Cyniak, H. Sakurai and A. Kasprzak, *ChemPlusChem*, 2025, **90**, e202500426.

33 J. A. Carrazana-García, E. M. Cabaleiro-Lago and J. Rodríguez-Otero, *Phys. Chem. Chem. Phys.*, 2017, **19**, 10543–10553.

34 D. Vijay, H. Sakurai, V. Subramanian and G. N. Sastry, *Phys. Chem. Chem. Phys.*, 2012, **14**, 3057.

35 U. D. Priyakumar, M. Punnagai, G. P. Krishna Mohan and G. N. Sastry, *Tetrahedron*, 2004, **60**, 3037–3043.

36 U. D. Priyakumar and G. N. Sastry, *Tetrahedron Lett.*, 2003, **44**, 6043–6046.

37 S. N. Spisak, Z. Wei, A. Yu. Rogachev, T. Amaya, T. Hirao and M. A. Petrukhina, *Angew. Chem. Int. Ed.*, 2017, **56**, 2582–2587.

38 J. Ażgin, S. Kulczyk, H. Sakurai, W. Wróblewski and A. Kasprzak, *J. Mater. Chem. C*, 2025, **13**, 16937–16945.

39 J. S. Cyniak, H. Sakurai and A. Kasprzak, *Chem. Eur. J*, 2025, e202500705.

40 J. Han, Y. Yakiyama, Y. Takeda and H. Sakurai, *Inorg. Chem. Front.*, 2023, **10**, 211–217.

41 J. S. Cyniak, D. Szeląg, R. Sitek, W. Wróblewski and A. Kasprzak, *J. Org. Chem.*, 2026, **91**, 4945–4961.

42 R. Stangenberg, D. Türp and K. Müllen, *Tetrahedron*, 2014, **70**, 3178–3184.

43 R. Guo, S. Ye, Y. Wang, Y. Duan, K. Di and L. Wang, *J. Mater. Chem. C*, 2021, **9**, 13392–13401.

44 S. Gupta, B. Basu and S. Das, *Tetrahedron*, 2013, **69**, 122–128.

45 T. R. Chan, R. Hilgraf, K. B. Sharpless and V. V. Fokin, *Org. Lett.*, 2004, **6**, 2853–2855.

46 R. Misra, R. Sharma and S. M. Mobin, *Dalton Trans.*, 2014, **43**, 6891.

47 A. D. Becke, *J. Chem. Phys.*, 1993, **98**, 5648–5652.

48 R. Krishnan, J. S. Binkley, R. Seeger and J. A. Pople, *J. Chem. Phys.*, 1980, **72**, 650–654.

49 C. Harriswangler, A. Freire-García, S. Argibay-Otero, A. Rodríguez-Rodríguez, J. M. Rodríguez, D. Esteban-Gómez, E. M. Vázquez-López, C. Platas-Iglesias, *Coord. Chem. Rev.*, 2025, **529**, 216434.

50 http://supramolecular.org/.

51 P. Thordarson, *Chem. Soc. Rev.*, 2011, **40**, 1305–1323.

52 D. Brynn Hibbert and P. Thordarson, *Chem. Commun.*, 2016, 52, 12792–12805.

View Article Online
DOI: 10.1039/D6CC02933G

Data availability

The data supporting this article have been included as part of the supplementary information.